

EXPERIMENTAL AND NUMERICAL INVESTIGATION OF HEAT TRANSFER AND PRESSURE DROP IN STAGGERED ARRANGEMENT HELICALLY FINNED-TUBE BUNDLE

Jiangtao YU, Di Liu, Wenxi Tian, M Y Zheng, Yingwei Wu, G H SU, and S Z Qiu*

School of Nuclear Science and Technology, Xi'an Jiao Tong University

28 Xianning West Road, Xi'an 710049, China

wxtian@mail.xjtu.edu.cn, yujiangtao0210@stu.xjtu.edu.cn

ABSTRACT

In a new pressurized water reactor nuclear power plant, the heat exchange tube bundle of the Moisture Separator Reheater (MSR) is a new designed staggered arrangement low helically finned-tube bundle.

To investigate the thermal hydraulic characteristics of the Reheater part of MSR, the tube bundle test section was designed by using prototype tube and prototype arrangement of the new designed MSR. The experiment was carried out on the test section with steam cross-flowing outside the horizontal tube bundle, same conditions as MSR' operation designing, and electrical heating in the tubes simulating the condensation heat release of the two phase-flow inside. A lot of experimental data on heat transfer and pressure drop were obtained in a broad experiment parameters range of wall heat flux density and steam temperature, pressure and Reynolds number. Based on the present data, empirical average heat transfer correlation and friction factor correlation were proposed for the outside average heat transfer and pressure drop. Comparisons and analysis between these experimental results and some of other investigations were made. The conclusions of this experimental investigation were given. The results are very useful to the design of the heat exchange tube bundle in the MSR, and the validations of the new design.

However, experimental studies cannot adequately reveal the detail of flow characteristics, and suitable correlations for this fin geometry are very rare. Thus, numerical simulations should be performed to make up for the deficiency. To perform a detail understanding of the heat transfer and pressure drop characteristics, a three-dimensional geometry was carefully constructed and a fine mesh was generated. The flow across the tubes was assumed to be a steady, incompressible turbulent flow. RNG based $k - \epsilon$ turbulence model was chosen in the simulation. Nusselt number and Euler number of a wide range of Reynolds numbers (based on the steam velocity through the minimum flow area) from 1×10^4 to 8×10^4 were calculated by the CFD software ANSYS Fluent. The numerical results were compared with experiment results of the same fin geometry and tube configuration. Also, local flow behavior and local temperature distribution were obtained to show the detail flow features and heat transfer. The velocity and temperature distribution near the fin surface were discussed

KEYWORDS

Steam cross-flow low helically finned-tube bundle; Experimental average heat transfer and friction factor correlations; Three-dimensional finned-tube numerical simulation

* Jiangtao YU, male, born in 1989, PhD student of School of Nuclear Science and Technology, Xi'an Jiao Tong University.

1. INTRODUCTION

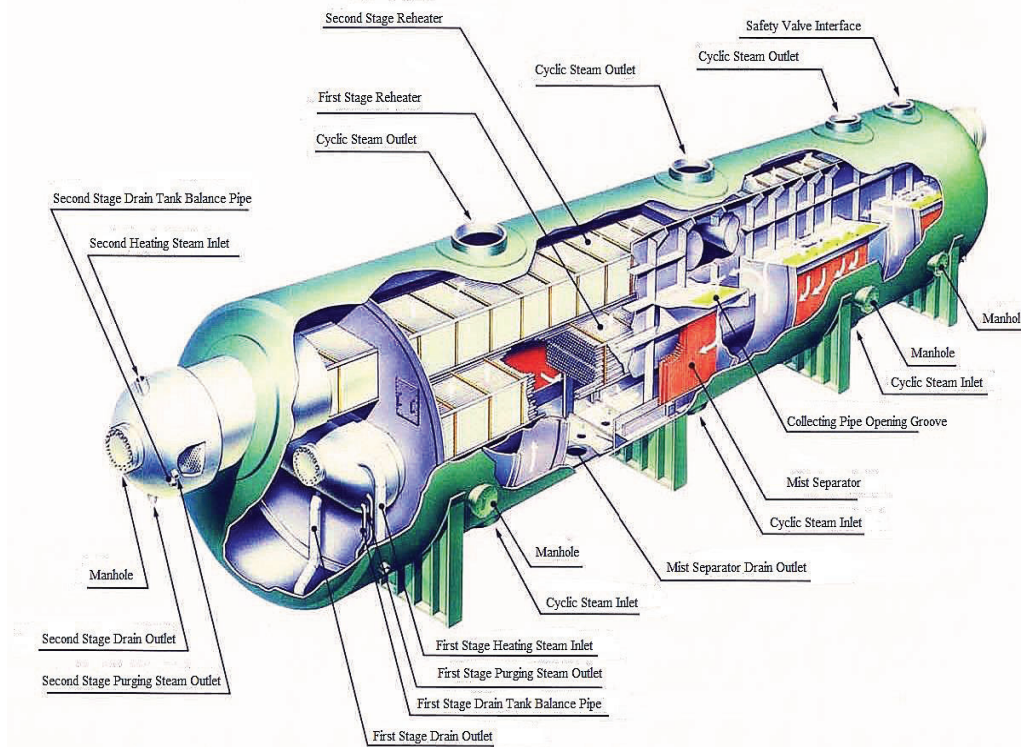


Figure 1.1. Model of Moisture Separator.

The Moisture Separator Reheater (MSR) is an important equipment of the Large Advanced PWR. Two MSR's are laid out in pair on both sides of the steam turbine in the conventional island, used to improve the safe and economic operation level of the steam turbine unit. The two main function parts of the MSR are the Mist Separator and the Reheater as shown in Fig. 1.1. Steam with humidity nearly coming to 14%, leaving from the last stage of the high-pressure turbine, is led into the MSR. According to the design, most part of the moisture in the steam will be separated by the Mist Separator. After the separation of the Mist Separator, the humidity of the steam entering up stage to the Reheater will be less than 1%. The Reheater consists of two stages of finned-tube bundles, the First Stage and the Second Stage, which is shown in Fig. 1.1.

As shown in Fig. 1.2, tubes of the Reheater are one kind of stainless steel material tubes with low fin height h_f and small fin spacing s_f helical fins outside and smooth surface inside. The tubes are compactly equilateral triangle staggered arranged. There are 26 rows of tubes in the First Stage, 28 rows in the Second Stage. Low-temperature saturated steam coming from the Mist Separator flows in shell side of the Reheater. High-temperature steam with humidity, coming from the exhaust steam at certain location in the high-pressure turbine for the First Stage or saturated steam from the Steam Generator for the Second Stage, flows in tube side. The low-temperature steam will be heated to superheated stage by the high-temperature steam inside the tubes, and then leaves the MSR for the low-pressure turbine to push the turbine to work, while the humidity of the high-temperature steam is increasing gradually along the tube pass. The schematic diagram of the system is shown as Fig. 1.3[1]. The reheat cycle consisting of mist separation and superheating in the turbine expansion process will contribute to a rise in turbine mechanical efficiency, and protect the high-speed circumferential blade from being damaged by the plenty of high speed water droplets.

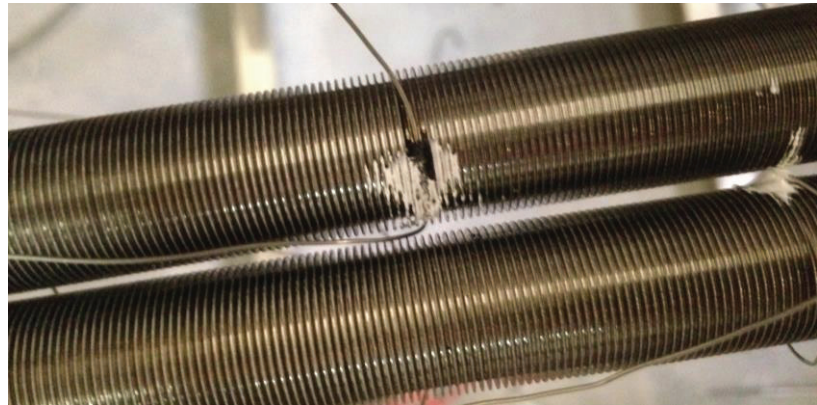
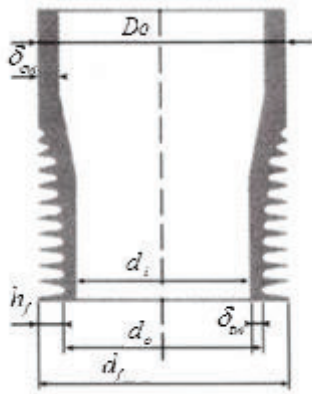


Figure 1.2. Finned-tube of the Reheater.

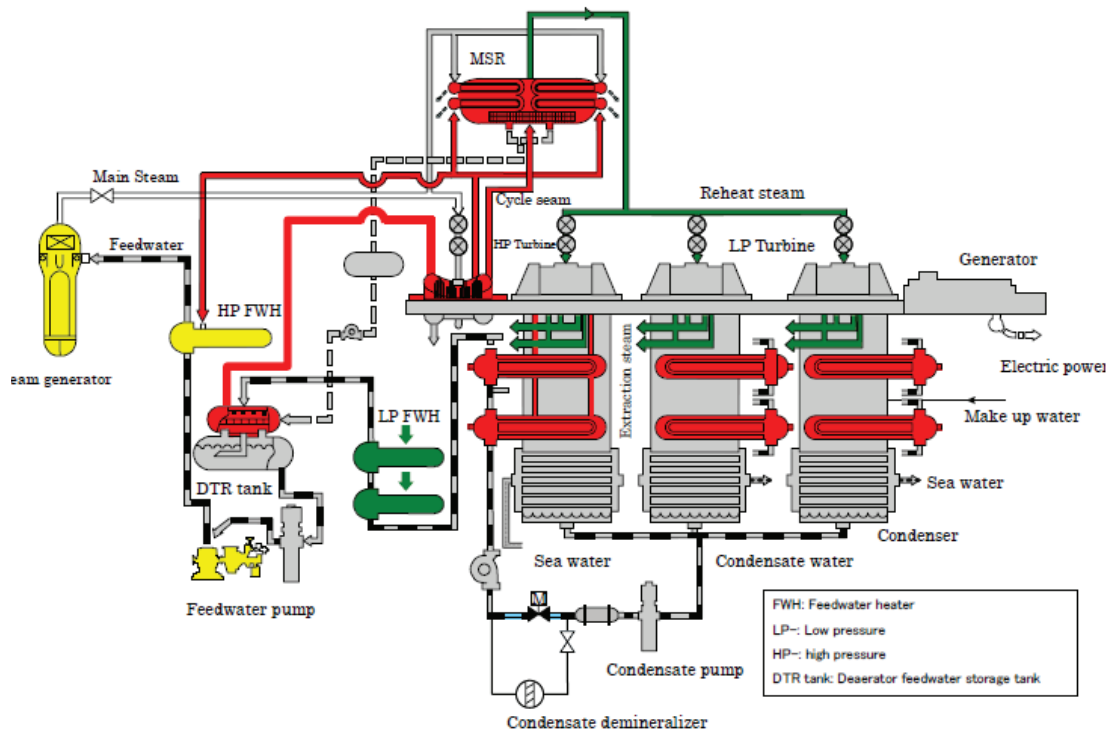


Figure 1.3. System and Equipment.
(Originated from the Journal of Power and Energy Systems, Vol.3, No.2, 2009, p369.)

Investigation of the outside tube average heat transfer and flow characteristics in the MSR bundle, under the operating condition steam flow medium, is very significant for the design of the Large Advanced PWR MSR. The purpose of this paper is to present a preliminary heat transfer and pressure drop correlations based on the experimental data, which can be used for this finned tube bundle. The finned-tube bundles are commonly used in the industries. A large number of experimental investigations have been carried for the circular and helically finned-tube bundles under the cross flow conditions and numerous heat transfer correlations and pressure drop correlations developed [2-8]. The heat transfer coefficient h and the pressure drop Δp are closely governed by the geometric of the bundle and the cross flow condition. Ward and Young [2] investigated on the heat transfer and pressure drop characteristics of

equilateral-triangular-pitch tube banks containing smooth integral helically finned tubes with air drawn by forced convection in cross flowing through seven finned tubes banks, then Briggs and Young [3] developed the investigation with nine additional banks and improved the heat transfer correlation and pressure drop correlation. Briggs and Young's correlation is widely accepted and used because of their investigation based on the widest range of parameters [4]. Webb [5] presented a survey of the existing correlations, recommending the heat transfer correlation of Briggs and Young [3] and the pressure drop correlation of Robinson and Briggs [6]. Nir [7] provided a quantitative comparison of some experimental data with the Briggs and Young's correlation, finding that the available heat transfer data of the plain finned-tube banks covered in $\pm 20\%$ of the results of the correlation of Briggs and Young [3]. Then Nir also presented a developed set of correlations of heat transfer and pressure drop in the finned-tube bundle cross flow based on his own experimental and 16 available sources. The finned-tubes used in the Nuclear Power plants moisture Separator Reheaters are low-finned tubes commonly. T.J. RABAS et al [8] studied on the low-finned tube bundles on two types of finned tubes, and presented a low-fin heat transfer correlation with additional data from five other sources then RABAS also presented a new low-fin friction factor correlation because he found that "the existing friction factor correlations were not successful in predicting these new pressure drop results."

The investigations in the past 80s of the heat transfer and pressure drop over finned-tube banks were practically taken under low temperature gas flow. The study of high temperature steam cross flowing the low finned-tubes were rarely seen. This experiment was carried out with superheated steam cross-flowing outside the horizontal low-finned-tube bundle, same conditions as MSR' operation design, and electrical heating in the tubes simulating the condensation heat release of the two phase-flow inside the tubes. The experiment research of this low-finned-tube bundle will be very useful for the development of the investigation concerned with the heat transfer and pressure drop characteristic for finned-tube bundle. For that this experiment is aim at the prototype tube and prototype arrangement of the new designed MSR, it will be significant for the research and design of the China Large Advanced PWR Program.

However, suitable correlations for this fin geometry are very rare, and experimental results cannot reveal the details of flow characteristics. To provide better understanding of the heat transfer and flow characteristics, numerical simulations should be performed. Mi Sandar Mon and Ulrich Gross [9] investigated the velocity and temperature distributions between the fins of four-row annular-finned tube bundles numerically. You Qin Wang et al [10] simulated turbulent flow through a staggered tube bank using computational fluid dynamics code FLUENT. C. Liang and G. Papadakis [11] used Large Eddy Simulation to study cross-flow through a staggered tube bundle. In this paper, the flow across the tubes was assumed to be a steady, incompressible turbulent flow. RNG based $k - \epsilon$ turbulence model was chosen in the simulation. Nusselt number and Euler number of a wide range of Reynolds numbers (based on the steam velocity through the minimum flow area) from 1×10^4 and 8×10^4 were calculated by the CFD software ANSYS Fluent.

2. EXPERIMENTAL APPARATUS AND PROCEDURE

The Large Flow Rate Steam Test Loop (LAFLOST) of XI'AN JIAOTONG UNIVERSITY Nuclear Thermal-hydraulic Laboratory (XJTU-NuThel), which was based on thermal power plant auxiliary steam system and capable of the output of 1.2 MPa and 20 tons per hour superheated steam or saturated wet steam, was designed for investigation of high pressure and high Re steam or two-phase flow thermal-hydraulic problems in nuclear reactors. LAFLOST was also capable to instrument the study of heat transfer and pressure drop, steam void friction and other problems concerning with the performance of steam-water two phase flow. In the present work, a finned-tube bundle test section was constructed, according to the prototype tube and prototype arrangement of the new designed MSR. The steam

experimental bench was set up to supply superheated steam for the test section. The experimental bench was illustrated in Fig. 2.1 and 2.2, and the test section Fig. 2.3.

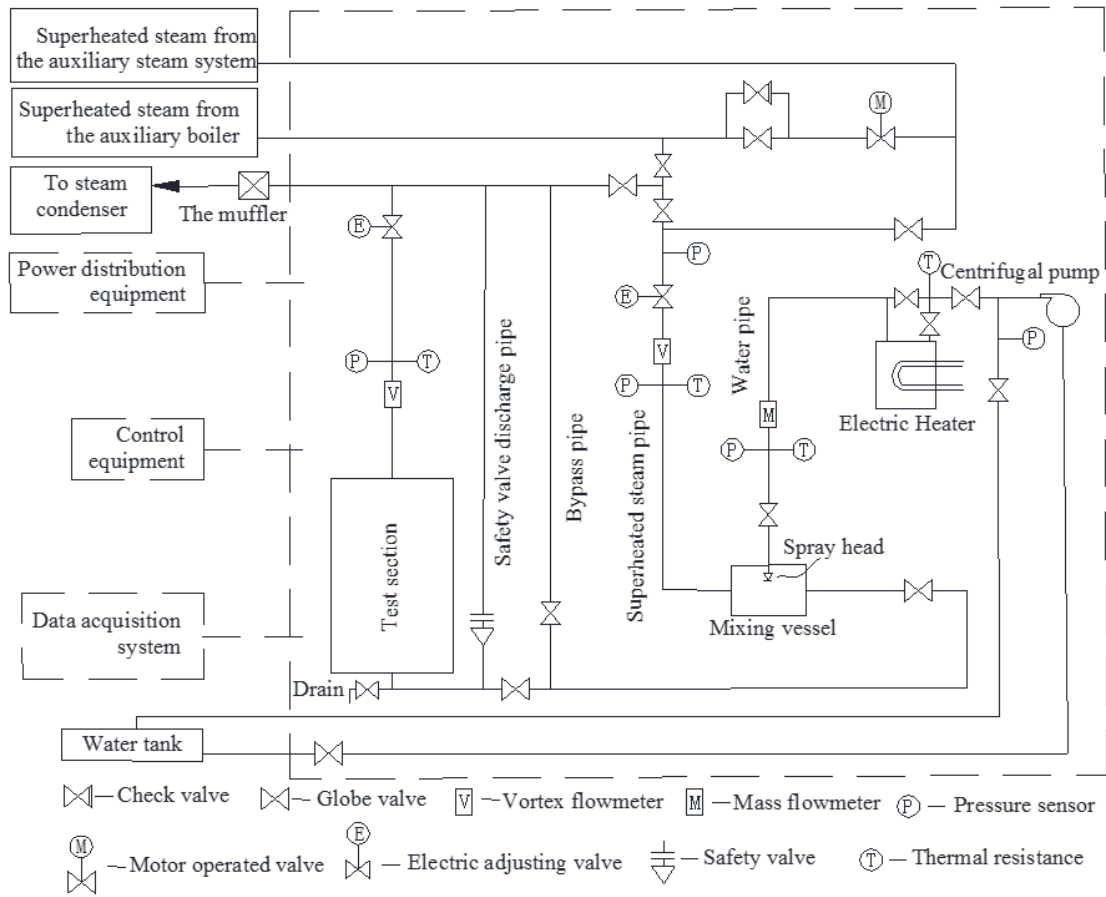


Figure 2.1. Schematic Diagram of the Experimental Bench.



Figure 2.2. Scene Photos of the Experimental Bench.

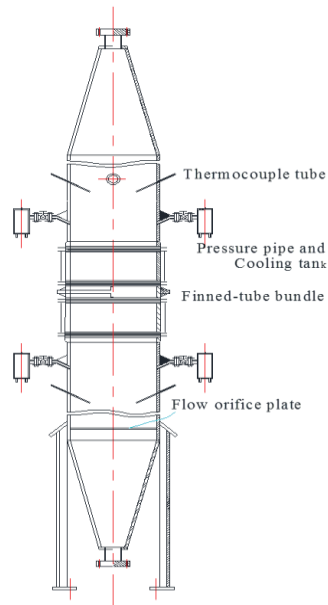


Figure 2.3. Test Section.

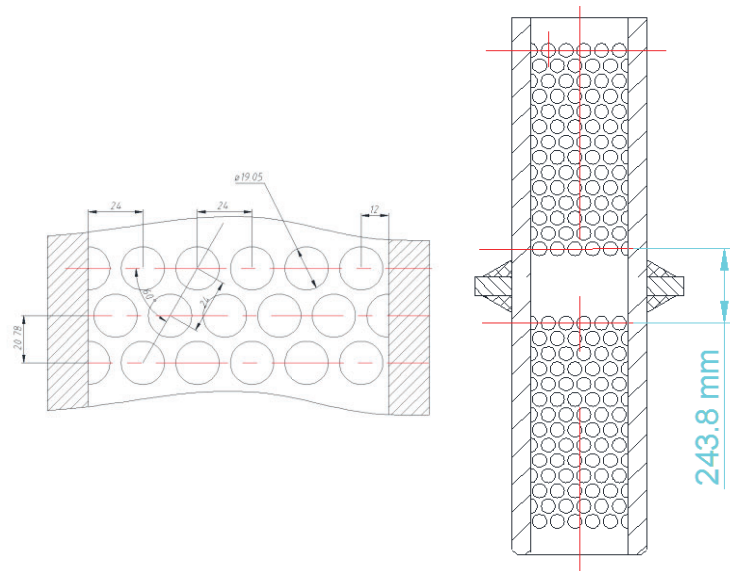


Figure 2.4. Tube Bank of the Test Section.

Superheated steam from the auxiliary steam system was generally rated at 0.7 MPa , $300\sim 350^{\circ}\text{C}$, and superheated steam supplied by the auxiliary boiler was rated at $0.7\sim 1.2\text{ MPa}$, 280°C . The two steam sources were selected for deferent test pressure demanded. The pressure and flow of the steam were regulated by the valves coupled adjustment. The volume flow of the superheated steam from the steam source was measured by a vortex flowmeter with measurement uncertainty of 0.5%, and the temperature of the steam was measured by a thermal resistance (pt-100 Ω) within accuracy of 0.5°C , the pressure of the steam was detected by a pressure transducer within the precision of 0.1%, readings to 0.1 Pa . The mass flow and the enthalpy flow of the steam could be calculated and derived. The water from the water tank was supplied by a centrifugal pump, and the pressure and flow of the water were regulated by the valves coupled adjustment too. The water mass flow was measured by a Coriolis force mass flowmeter with measurement uncertainty of 0.2%. The water temperature was measured by a thermal resistance (pt-100 Ω) within accuracy of 0.5°C . The pressure of the water was detected by a pressure transducer within the precision of 0.1%. The mass flow and the enthalpy flow of the water could be calculated and derived then. If the temperature of the steam was too high, the centrifugal pump would be started to spray water into the steam to cool the steam by a spray head.

After the mixing vessel, the steam was cooled down to the temperature needing by the test. Steam entered the test section gradually expanding in the entrance section. The steam flow field was homogenized basically after the flow orifice plate assembled before the core region. The temperature and the pressure of the steam upstream of the finned-tube bundle was respectively measured by a pair of thermocouples deep of 16 cm and faced into the incoming steam stream within accuracy of 0.5°C , a pressure transducer connecting the tube of the steam cooling tank within the precision of 0.1% and adjusted range of 0 to 1.5 MPa . The temperature and the pressure of the steam downstream of the finned-tube bundle was detected similar of the upstream. The pressure drop of the steam cross flowing the bundle was detected by a pair of differential pressure transmitter within accuracy of 0.1% and range of -20 to 20 KPa . The volume flow of the superheated steam flowing through the test section was measured by a vortex flowmeter with measurement uncertainty of 0.5%, and the temperature of the steam was measured by a thermal resistance (pt-100 Ω) within accuracy of 0.5°C , the pressure of the steam was detected by a pressure transducer within the precision of 0.1%, readings to 0.1 Pa .

There were 28 rows with 5 tubes per row in the bundle bank, 140 tubes in total. In order to simulate an ideal tube bundle, half-tubes without heating inside were attached to the sidewalls in the whole bundle, as shown in Fig. 2.4. The detailed geometrical parameters of the finned-tube bundle configuration was tabulated in Fig.2.5 and Table 2.1. The half-tubes were made from the same finned-tube of the bundle by saw cutting along the tube longitudinal centerline. There was an electric heating rod, diameter of 13.8mm and heating section long of 500mm, assembled in per tube of the bundle, as shown in Fig. 2.5. The 140 electric heating rod were the same specification, and the heat rate in the tube was determined and adjusted by the voltage on the rod resistance. The power supply of the electric heating rods was controlled and adjusted by the voltage regulators. The heat rate of the tube for every test condition approached the heat transfer rate of the corresponding MSR operate condition. There were 112 thermocouples regularly arranged in 28 ones of the 140 tubes. Longitudinal grooves deep 0.5mm, wide 0.7mm and long 250mm were engraved on the inside wall of the tubes to set thermocouples. The longitudinal grooves on the inside wall were against, side facing and back facing the steam flow. The inside wall temperature of the tube was measured by the thermocouples in the grooves. All the walls of the steam pipes and the test section walls were insulated with 15cm aluminum silicate fiber, and the heat loss of the test section walls was less than 5% as estimated.

Table 2.1. The detailed geometrical parameters of the finned-tube bundle configuration.

d_i (mm)	14.31	d_o (mm)	16.51	A_o (m^2)	0.1021
d_f (mm)	19.05	h_f (mm)	1.27	A_f (m^2)	0.0817
δ_f (mm)	0.2	θ_f	4'	6.250×10^{-3}	1.563×10^{-3}
s_f (mm)	0.941	S_t (mm)	20.78	A_t (m^2)	0.0204
S_l (mm)	12.0	n	28	A_{min} (m^2)	0.0209
n_r	5	N	140	Tube Material	Stainless Steel
L (mm)	500	A_i (m^2)	0.0225	λ ($Wm^{-1} \circ C^{-1}$)	25.4

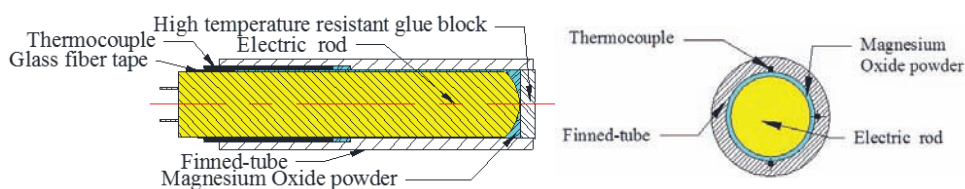


Figure 2.4. Electric Heating Rod and Thermocouple Assembled in Tube.

Before the whole experiment, the water gathered in the steam pipe system and the test section should be discharged by the drain pipe. The steam pipe system needed a slowly warming by procedure then. For a certain test condition, steam sources were selected for the test condition pressure requirements. The pressure, mass flow and temperature of the steam entering the test section could be adjusted to the appropriated value by the regulation of the valves on the steam pipes and the water flow rate spraying to the steam. Later on, heat rate of the electric rod in the tubes was gradually raised to meet the test condition requirement. The temperature of the steam and the inside wall both rise slowly and tended to be stable after a few minutes then. The steady state condition for the test was determined by the variation

amplitudes of the downstream steam temperature and mass flow rate, with temperature variation amplitudes in $0.5^{\circ}C$ per minute and flow rate variation amplitudes 1% per minute. All the data signals were collected and converted by the data acquisition system all the time, by an acquisition of 10 times per second and display frequency of 2 times per minute, when the tests was being carried, and the converted signals will be transmitted to the host computer for observation and operation. Particularly, the data signals on the steady state condition would be recorded continuously not less than 5 minutes in an excel file for further analysis. After one test, the entrance steam condition and the heat rate of the tubes would be regulated to meet another test conditions.

3. NUMERICAL SIMULATION

The heat transfer and flow in finned tube bank was modeled as three-dimensional periodic heat flow. The computational domains of the proposed staggered finned-tube bundles were sketched by dotted lines, shown in Fig. 3.1. The symmetry boundaries and periodic boundaries were labeled. In the periodic heat transfer, the temperature change between periodic boundaries is constant. After checking the grid independence, the grid with 280,000 cells was used. The max near wall $y+$ was 6.5. Standard $k-\epsilon$ model and enhanced wall treatment were selected in the numerical simulation. The properties of steam were calculated by the measured temperature and pressure in the experiment. The periodic boundaries was set in the FLUENT. In the periodic conditions, mass flow and upstream bulk temperature was specified according to the measured data in the experiment. The boundary conditions of fins were non-slip wall, and the temperature was that measured in the experiment. COUPLED algorithm in FLUENT was used. The gradient was discretized by least squares cell based method. All other governing equations were discretized by QUICK method. Pseudo Transient algorithm in the coupled pressure-based solver was enabled.

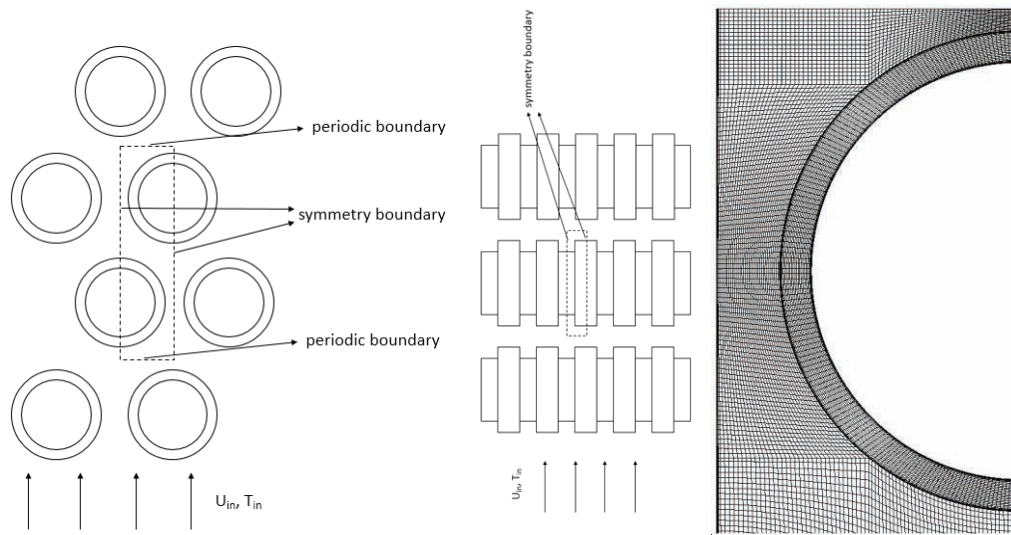


Figure 3.1. Computational Domains and CFD grids of the Finned-tube Bundles.

A numerical simulation result of the CFD was shown at Fig.3.2, Reynolds number of this result was 34000, the temperature and the velocity distribution of the steam could be seen from the figures. The boundary layer separation on the tube near the fin surface plane occurred at about 60° . For a row middle of the tube bundle, heat transfer at stagnation point of the tube near the fin surface plane was the strongest and temperature of steam there was the lowest. From the upstream facing region of the tube, the velocity of the steam increased with the decrease of flow section. After the minimum flow section place, heat

transfer of where the boundary layer separation occurring was the lowest and the temperature of steam from the layer separation to the back point was rising first and down then, for the vortices occurring and developing. The overall heat transfer coefficient and pressure drop could be obtained by the CFD then. The range of Re for all the experiment and simulation conditions was from 11000 to 75000. So these steam flow conditions of the experiment tests and simulation results were all fully developed turbulent flows and their flow phenomena were similar.

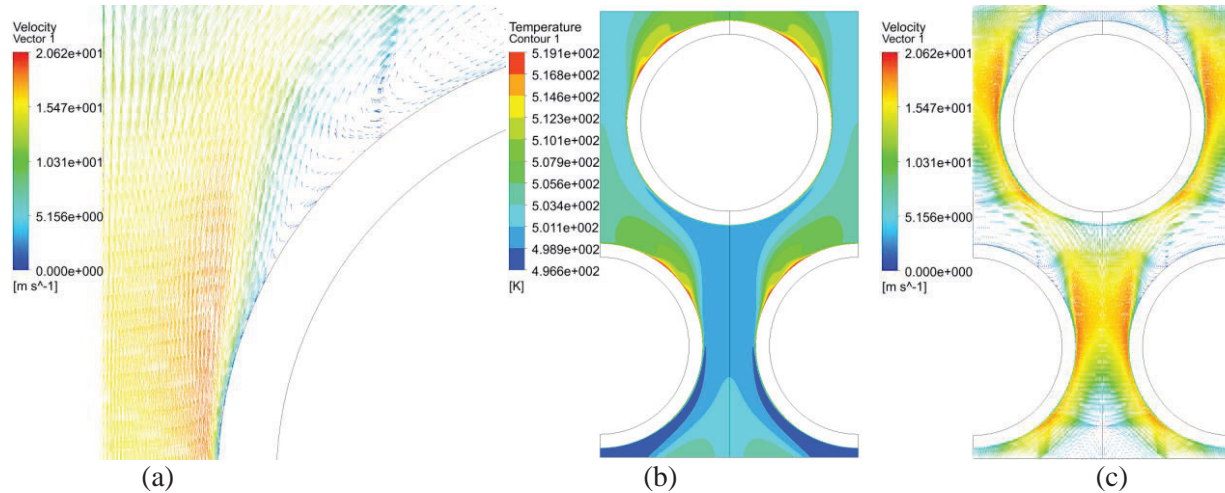


Figure 3.2. Velocity and Temperature Distribution near the Fin Surface Plane at $Re=31500$ and $T_i = 519K$.

(a. Convection Boundary Layer Development and Separation; b. Temperature Distribution; c: Velocity Distribution.)

4. ANALYSIS OF THE TEST DATA

All the physical properties used in this paper was computed by the authoritative software REFPROP.

The average convective heat transfer coefficient of bundle was

$$h = \frac{\Delta HW}{N\eta_0 A_0 \Delta T} \quad (4.1)$$

The total number of the tubes was $N = 140$, and the total area of tube out surface $A_o = 0.1021mm$.

For one tube with thermocouples inside, because the inside wall temperature of the tube T_i was measured by the thermocouples in the grooves, the outside wall temperature T_o would be corrected for conduction drop through the wall. This was accomplished by using the flowing equation (4-2) to (4-4) for cylinder wall heat conduction:

$$\frac{\Delta t}{\Phi} = \frac{\ln(d_o / d_i)}{2\pi\lambda l_h} \quad (4.2)$$

$$\Phi = \frac{U^2}{20.16667} \quad (4.3)$$

$$T_o = T_i - \Delta t \quad (4.4)$$

The electric power of all the 140 tubes were same at every test condition. The value of inside wall temperature of every tube T_i was obtained by averaging the values of the several thermocouples functioning normally inside the tube.

The outside wall mean temperature of all the tubes \bar{T}_o was obtained by arithmetical averaging of the values of all the reasonable T_o .

The bulk mean temperature of the steam T_A used to calculate the physical property of the steam was defined as

$$T_A = (T_U + T_D) / 2 \quad (4.5)$$

The heat transfer temperature difference $\Delta T = (\bar{T}_o - T_A) / 2$ used in the equation (4-1) was defined as

$$\Delta T = (\bar{T}_o - T_A) / 2 \quad (4.6)$$

The overall fin efficiency η_0 was defined as

$$\eta_0 = \frac{A_r + \eta_f A_f}{A_r + A_f} \quad (4.7)$$

η_f was the single fin efficiency can be derived depending on the Harper-Brown assumption[11][12]:

$$\eta_f = \frac{2r'}{\varphi(1+r')} \cdot \frac{I_1(\varphi R_1)K_1(\varphi R_0) - K_1(\varphi R_1)I_1(\varphi R_0)}{I_0(\varphi R_0)K_1(\varphi R_1) + K_0(\varphi R_0)I_1(\varphi R_1)} \quad (4.8)$$

$$\varphi = \sqrt{2h_f(r_2 - r_0)^3 / (\lambda_f \delta_f)} \quad (4.9)$$

$$r_2 = r_1 + \delta_f / 2 \quad (4.10)$$

$$r' = r_0 / r_2 \quad (4.11)$$

$$\varphi R_1 = \varphi / (1 - r') \quad (4.12)$$

For the above equations from (4-8) to (4-12), η_0 would be obtained by iterative calculation.

The steam enthalpy rise ΔH was defined as

$$\Delta H = H_D - H_U \quad (4.13)$$

H_U and H_D were the total vapor enthalpy respectively of the upstream steam and the downstream steam corresponding to their temperature, pressure and mass flow.

By the Chilton-Colburn analogy [13] for the Prandtl numbers in the range, the functional relationship of the finned-tube bundle heat transfer $Nu = \Phi(\text{Re}, \text{Pr})$ suggested by the governing equations became

$$Nu = C \text{Re}^m \text{Pr}^{1/3} \quad (4.14)$$

The Nu number and the Re number were defined as

$$Nu = hd_0 / \lambda \quad (4.15)$$

$$\text{Re} = u_{\max} d_o / \nu \quad (4.16)$$

The pressure drop was expressed in the dimensionless form by Euler number

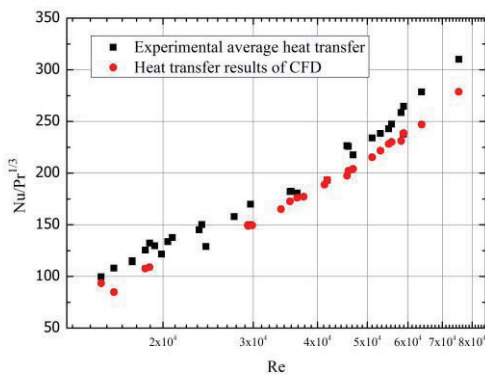
$$Eu = \frac{2\Delta P}{\rho u_{\max}^2} \quad (4.17)$$

5. RESULTS AND DISCUSSIONS

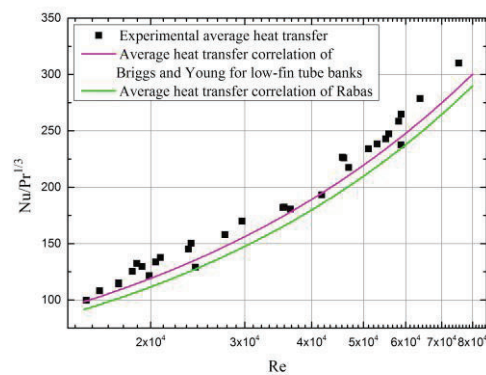
The main purpose of this investigation was to determine the heat transfer and pressure drop correlations for this finned tube bundle which would be valid for the design of the Large Advanced PWR MSR.

5.1. HEAT TRANSFER

Since the Prandtl number of the superheated steam for all the experiment data varied slightly, and the Reynolds number was the most important variable in the heat transfer correlation equation. The dependent variable for the regression analysis was taken as $Nu/Pr^{1/3}$, the bulk temperature viscosity and the wall temperature viscosity ratio $[\mu/\mu_w]^{0.25}$ was approximately 0.985 for all the experimental data and excluded in the correlation equation. And the bulk temperature Prandtl number and the wall temperature Prandtl number ratio was $(Pr/Pr_w - 1) \leq 0.007$ for all the experimental data, so the difference between film heat transfer coefficient based on the film temperature properties and average heat transfer coefficient based on the bulk temperature properties was very small.



Figures 5.1. Comparison of the heat transfer coefficients for experiment and CFD.



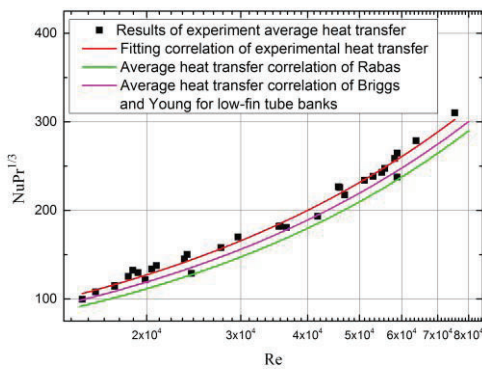
Figures 5.2. Comparison of the heat transfer coefficients between the experiment data and the available correlations.

Figure 5.1 presented the comparison of the average heat transfer coefficients for experiment and CFD, the results of experiment and CFD were corresponding very well in trend, but with about 10% higher than the CFD, which may be because of the method of CFD. A more detailed presentation on the reason of heat transfer difference results between experiment and CFD might be presented at a later date. Figure 5.2 presents the comparison of the heat transfer coefficients for experiment and two available correlations. Generally, the results of experiment actually rose slightly up the correlation presented by Rabas et al [8] and the correlation for the low-fin tube banks presented by Briggs and Young [3]. For the fin height of the experiment finned tube was lower than any one of the finned tubes investigated by Rabas et al and Briggs et al. Figure 5.3 presented the fitting line and comparison of the correlations of [8] and [3]. From Figures 5.2 and 5.3, it could be noticed that the difference between the experiment heat transfer data and these two available suitable correlations was very small, and for the geometrical characteristic of this experiment finned tube bank was very similar to that of Rabas et al [8], the heat transfer performance of

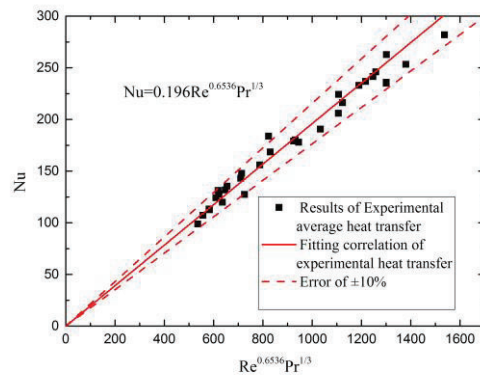
this experiment new tube bank was much more close to that of Rabas et al [8]. Figure 5.4 showed the errors of the fitting results to the experiment data, and all the fitting errors were within $\pm 10\%$. So the heat transfer correlation of the experiment tube bundle for $1 \times 10^4 < Re < 8 \times 10^4$ was presented as:

$$Nu = 0.196Re^{0.6536}Pr^{1/3} \quad (5.1)$$

In the experiment, the measurement accuracy of the inner wall temperature of finned-tube T_i had great influence on the heat transfer results. Because the axial heat flux density was great and the tube diameter was small. The temperature of electric heating rod wall was very high, about 100-200 °C higher than the temperature of the steam observed from the test data. There was a great heat flux density between the rod wall and the tube inner wall, which might cause possibility of errors on the measuring of the tube inner wall temperature. Some of the experiment data diffused in a range but not bigger than $\pm 10\%$ seen from Fig. 5.4.

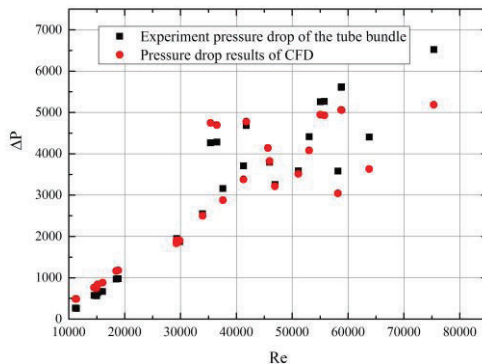


Figures 5.3. Fitting of the heat transfer coefficients for experiment and comparison with the available correlations.

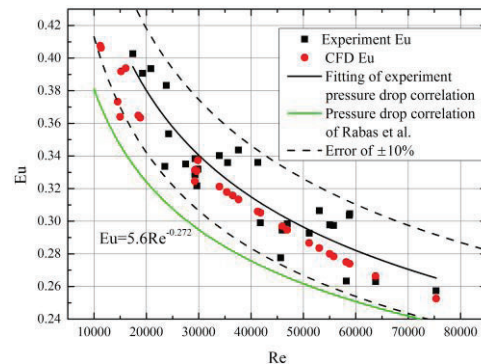


Figures 5.4. Fitting results of the heat transfer coefficients and errors of the fitting.

5.2. PRESSURE DROP



Figures 5.5. Comparison of experiment and CFD for pressure drop.



Figures 5.6. Comparison and fitting of pressure drop.

Figure 5.5 presented the variation of the experiment pressure drop ΔP and comparison to the results of CFD. The CFD results had a similar trend with the experiment data. Figure 5.6 presented the comparison and fitting of pressure drop. The correlation of Rabas et al [5] fell slightly below the results of this experiment Eu. It was suitable to recommend the pressure drop correlation for $1 \times 10^4 < Re < 8 \times 10^4$ fitting based on the experiment for the superheated steam flowing through this kind of finned-tube bundle at present:

$$Eu = 5.6Re^{-0.272} \bullet n \quad (5.2)$$

6. CONCLUSION

Experimental measurements of heat transfer and pressure drop of superheated steam cross flowing this equilateral-triangular pitch low helically finned-tube bundle were carried, with same conditions as MSR' designing operation and electrical heating in the tubes simulating the condensation heat release of the two phase-flow inside. Three dimensional numerical simulations on the experiment corresponding conditions were calculated by the CFD software ANSYS Fluent. Results of the experiment and CFD for average heat transfer were compared together with the results of Rabas et al [8] and Briggs and Young [3]. The average heat transfer correlation for the experiment condition was proposed. The pressure drop results of the experiment and CFD are presented and compared with the Rabas et al [8]. The non-isothermal pressure drop correlation based on this experiment was proposed too.

NOMENCLATURE

A_f Total area of the fins (m^2)	H_U Enthalpy of the steam upstream (J)
A_{min} Minimum flow area of the bundle (m^2)	H_D Enthalpy of the steam downstream (J)
A_i Tube inner surface area (m^2)	I_0 The zero order modified Bessel function of the first class
A_o Total area of the finned tube surface (m^2)	Nu Nusselt number
A_t Tube outer surface root area between fins (m^2)	I_1 The first order modified Bessel function of the first class
d_i Inside diameter (m)	L Tube length (m)
d_o Outside diameter (m)	K_0 The zero order modified Bessel function of the second class
d_f Fin outer diameter (m)	K_1 The first order modified Bessel function of the second class
D_o Outer diameter of the original pipe	n Rows number
h Average convective heat transfer coefficient ($W \cdot m^{-2} \cdot ^\circ C^{-1}$)	ΔP Pressure drop through the tube bundle
G_m Mass velocity based on the minimum flow area	Re Reynolds number
Eu Euler number	s_f Fin spacing (m)
h_f Fin height (m)	S_l Longitudinal pitch (m)
h'_f Fin surface heat transfer coefficient ($W \cdot m^{-2} \cdot ^\circ C^{-1}$)	S_t Transverse pitch (m)
\bar{h} Average heat transfer coefficient ($W \cdot m^{-2} \cdot ^\circ C^{-1}$)	u_{max} The steam mass flow through the minimum flow area of the bundle ($kg \cdot m^{-2} \cdot s^{-1}$)
ΔH Steam enthalpy rise (J)	W Steam mass flow ($kg \cdot s^{-1}$)
	N Number of the tubes in total

Δt Temperature drop from the inside to outside wall ($^{\circ}\text{C}$)
 Pr Prandtl number
 T_o Temperature of tube outside wall ($^{\circ}\text{C}$)
 l_h length of the tube heating section (m)
 \bar{T}_o Outside wall mean temperature of all the tubes ($^{\circ}\text{C}$)
 T_U Bulk temperature of the steam upstream ($^{\circ}\text{C}$)
 T_D Bulk temperature of the steam downstream ($^{\circ}\text{C}$)
 T_A Bulk mean temperature of the steam ($^{\circ}\text{C}$)
 ΔT Heat transfer temperature difference ($^{\circ}\text{C}$)
 ρ steam density of average bulk temperature (kg/m^3)

η_f Single fin efficiency
 η_0 Overall fin efficiency
 Φ Electric power of the heating rod (W)
 U Voltage of the heating rod (V)
 r_o Fin root radius (m)
 r_i Fin head radius (m)
 R Resistance of the heating rod (Ω)
 δ_f Fin thickness (m)
 δ_{rw} Wall thickness of the base tube (m)
 δ_{ow} wall thickness of the original tube
 θ_f Fin cone angle
 λ Tube thermal conductivity ($\text{W}/\text{m}^{\circ}\text{C}$)
 λ_f Fin thermal conductivity ($\text{W}/\text{m}^{\circ}\text{C}$)
 ν Kinematic viscosity (m^2s^{-1})

REFERENCES

1. Jun MANNABE and Jiro KASAHARA, "Moisture Separator Reheater for NPP Turbines", *Journal of Power and Energy Systems*, Vol.3, No.2, 2009, p368-381.
2. Ward, D. J., and Young, E. H., "Heat Transfer and Pressure Drop of Air in Forced Convection across Triangular Pitch Banks of Finned Tubes," *Chemical Engineering Progress Symposium Series*, No. 29, Vol. 55, pp.37-44, 1959.
3. Briggs, D. E., and Young, E. H., "Convection heat transfer and pressure drop of air flowing across triangular pitch banks of finned tubes," *Chemical Engineering Progress Symposium Series*, No. 41, Vol. 59, pp.1-10, 1963.
4. Mi Sandar Mon, "Numerical Investigation of Air-Side Heat Transfer and Pressure Drop in Circular Finned-Tube Heat Exchangers," [D].Germany: Uni. Of Freiburg Mining Institute, 2003.
5. Webb, R. L., "Air-Side Heat Transfer in Finned Tube Heat Exchangers," *Heat Transfer Engineering*, Vol. 1, No. 3, pp.33-49, 1980.
6. Robinson, K. K., and Briggs, D. E., "Pressure Drop of Air Flowing Across Triangular Pitch Banks of Finned Tubes," *Chemical Engineering Progress Symposium Series*, No. 64, Vol.62, pp.177-184, 1965.
7. Nir, A., "Heat Transfer and Friction Factor Correlations for Cross Flow Over Staggered Finned Tube Banks," *Heat Transfer Engineering*, Vol.12, No. 1, pp. 43-58, 1991.
8. T.J. RABAS, P.W. ECKELS & R.A. SABATINO, "The Effect of Fin Density on the Heat Transfer and Pressure Drop Performance of Low-Finned Tube Banks," *Chemical Engineering Communications*, Vol. 10, Issue 1-3, 1981, pp. 127-147.
9. Mon, Mi Sandar, and Ulrich Gross, Numerical study of fin-spacing effects in annular-finned tube heat exchangers. *International Journal of Heat and Mass Transfer* 47.8 (2004): 1953-1964.
10. Wang, Y. Q. and P. Jackson, et al. (2006). Turbulent Flow through a Staggered Tube Bank. *Journal of Thermophysics and Heat Transfer* 20(4): 738-747.
11. Liang, C. and G. Papadakis (2007). Large eddy simulation of cross-flow through a staggered tube bundle at subcritical Reynolds number. *Journal of Fluids and Structures* 23(8): 1215-1230.
12. Harper, D. R., and Brown, W. B. (1922). *Mathematical Equations for Heat Conduction in the Fins of Air Cooled Engines*, NACA Rep. 158, National Advisory Committee on Aeronautics, Washington, DC.
13. Kraus A D, Aziz A, Welty J. *Extended surface heat transfer [M]*. Wiley.com, 1972. p182.